



Cirripede Cypris Antennules

How Much Structural Variation Exists Among Balanomorphan Species from Hard-Bottom Habitats?

Chan, Benny K. K.; Sari, Alireza; Høeg, Jens Thorvald

Published in:
Biological Bulletin

DOI:
[10.1086/695689](https://doi.org/10.1086/695689)

Publication date:
2017

Document version
Publisher's PDF, also known as Version of record

Document license:
[CC BY-NC](#)

Citation for published version (APA):
Chan, B. K. K., Sari, A., & Høeg, J. T. (2017). Cirripede Cypris Antennules: How Much Structural Variation Exists Among Balanomorphan Species from Hard-Bottom Habitats? *Biological Bulletin*, 233(2), 135-143.
<https://doi.org/10.1086/695689>

Cirripede Cypris Antennules: How Much Structural Variation Exists Among Balanomorph Species from Hard-Bottom Habitats?

BENNY K. K. CHAN^{1,*}, ALIREZA SARI², AND JENS T. HØEG³

¹*Biodiversity Research Center, Academia Sinica, Taipei 115, Taiwan;* ²*School of Biology and Centre of Excellence in Phylogeny of Living Organisms, College of Science, University of Tehran, Tehran, Iran;* and ³*Marine Biology Section, Department of Biology, University of Copenhagen, Universitetsparken 4, DK-2100 Copenhagen, Denmark*

Abstract. Barnacle cypris antennules are important for substratum attachment during settlement and on through metamorphosis from the larval stage to sessile adult. Studies on the morphology of cirripede cyprids are mostly qualitative, based on descriptions from images obtained using a scanning electron microscope (SEM). To our knowledge, our study is the first to use scanning electron microscopy to quantify overall structural diversity in cypris antennules by measuring 26 morphological parameters, including the structure of sensory organs. We analyzed cyprids from seven species of balanomorph barnacles inhabiting rocky shore communities; for comparison, we also included a sponge-inhabiting balanomorph and a verrucomorph species. Multivariate analysis of the structural parameters resulted in two distinct clusters of species. From nonmetric multidimensional scaling plots, the sponge-inhabiting *Balanus spongicola* and *Verruca stroemia* formed one cluster, while the other balanomorph species, all from hard bottoms, grouped together in the other cluster. The shape of the attachment disk on segment 3 is the key parameter responsible for the separation into two clusters. The present results show that species from a coastal hard-bottom habitat

may share a nearly identical antennular structure that is distinct from barnacles from other habitats, and this finding supports the fact that such species also have rather similar reactions to substratum cues during settlement. Any differences that may be found in settlement biology among such species must therefore be due either to differences in the properties of their adhesive mechanisms or to the way that sensory stimuli are detected by virtually identical setae and processed into settlement behavior by the cyprid.

Introduction

Barnacles are sessile marine organisms that occupy a vast range of marine habitats ranging from the coastal zone to the deep sea; and the species comprise well-known suspension feeders, numerous epibionts on a wide range of host organisms, and some of the most advanced parasites known from Metazoa (Anderson, 1994; Høeg and Møller, 2006; Rees *et al.*, 2014). All barnacles have free-swimming larvae, and settlement is accomplished by the highly specialized cyprid larval stage (Walker *et al.*, 1987; Glenner, 1999; Høeg *et al.*, 2004). Cirripedes have become favored organisms for the study of marine larval settlement because of their range of life forms, their ubiquity as biofoulers, and the structural diversity of juveniles formed by metamorphosis of the settled cyprid. At the light microscopical level, the morphology of the cyprid appears to be surprisingly similar throughout the entire taxon, but studies with the scanning electron microscope have shown significant variation in the structure of the antennules (Glenner *et al.*, 1989; Moyse *et al.*, 1995). This is hardly surprising because it is by means of these specialized appendages that the

Received 17 August 2017; Accepted 13 October 2017; Published online 12 January 2018.

*To whom correspondence should be addressed. E-mail: chankk@gate.sinica.edu.tw.

Abbreviations: AD, attachment disk; ANOSIM, analysis of similarity; as2, second antennular segment; as3, third antennular segment; nMDS, non-metric multidimensional scaling; RDS, radial disk setae; RDS-5, radial disk seta 5; SIMPER, similarity percentage; TS-A+B, terminal setae A and B; TS-D, terminal seta D.

Online enhancement: supplemental table.

cyprid first explores the substratum by bipedal walking and finally attaches by irreversible cementation (Walker and Yule, 1987; Lagersson and Høeg, 2002; Maruzzo *et al.*, 2011). To accomplish this critical task, the four-segmented antennules are equipped with an array of sensory organs and glands. The penultimate third segment is short and carries the so-called attachment disk (AD), which is a flat surface covered with cuticular villi onto which the glands terminate that are used in both temporary adhesion and final cementation. Almost all setae are also located either on this segment or on the small fourth segment, which projects from the side of the third segment and thus extends the area from which stimuli can be picked up; and they have all been shown to be sensilla (sensory setae) (Nott, 1969; Walker *et al.*, 1987; Lagersson and Høeg, 2002; Maruzzo *et al.*, 2011).

This introduces the question of whether structural diversity of the cypris antennule is correlated with the diversity of habitats and substrata used in settlement by cirripede species. With this aim, Al-Yahya *et al.* (2016) performed a morphometric analysis of the third segment (the attachment organ) in cyprids from a selection of barnacles inhabiting many different habitats. Significant variation was found among the investigated species, with respect to both the general shape of the segment and the structural details of the AD. Al-Yahya *et al.* (2016) suggested that the variation was related to the different substrata used by the species, but their analysis, based on very few structural parameters, could not adequately demonstrate this claim. Furthermore, the Al-Yahya *et al.* (2016) study was confined to the shape of the third segment and the structure of the AD, but it left unexamined the fourth segment, which contains a multitude of sensilla that play a key role in locating the settlement site (Walker *et al.*, 1987; Glenner *et al.*, 1989; Clare and Nott, 1994; Glenner, 1999; Blomsterberg *et al.*, 2004; Kolbasov and Høeg, 2007; Bielecki *et al.*, 2009).

Within cirripedes, species of acorn barnacles (Thoracica: Balanomorpha) inhabiting rocky shores are an ecologically very important group that often completely dominate their habitat, and they are also among the most damaging foulers of man-made objects in the sea (Bertness *et al.*, 1998; Thompson and Nagabhushanam, 1999). The study of Al-Yahya *et al.* (2016) suggests that these species share a number of characteristics not found in barnacles from other habitats. The third segment is symmetrically bell shaped, and it has a near circularly shaped AD surrounded by a so-called velum, a fringe of long and thin cuticular filaments. Al-Yahya *et al.* (2016) argued that these structural characteristics represent an adaptation to settlement on rocky bottoms in high-energy coastal zones. Unfortunately, there are few accounts that compare settlement biology among balanomorphan cirripedes. Some recent studies, cited by Di Fino *et al.* (2014), claim that some hard-bottom-inhabiting species react differently to settlement cues in the substratum, but Di Fino *et al.* (2014) themselves failed to find this when comparing settlement in cyprids of *Amphibalanus* (*Balanus*) *improvisus* and *Amphibalanus amphitrite*.

Here we perform a refined morphological analysis to investigate whether cyprids of balanomorphan barnacles from hard-bottom habitats possess similar antennular structure or vary in a way that could be correlated with differences in settlement biology. To our knowledge the present study is the first to use scanning electron microscopy to quantify variation in the entire structure of the cypris antennule. We study seven species of balanomorphan barnacles from rocky-bottom habitats. The taxonomy of the Balanomorpha is presently uncertain (Pérez-Losada *et al.*, 2008, 2014), but all of our species are confined to the balanomorphan superfamily Balanoidea, which serves to phylogenetically confine our selection. We measure 26 structural parameters in the antennules, including the setae, and subject them to analysis by multivariate statistics. For comparison, we also include one balananoidean species from an entirely different habitat, namely, epibiotic in marine sponges, and a species from the Verrucomorpha, which is the sister group to the Balanomorpha.

Materials and Methods

Larval culture and SEM preparation

We cultured larvae of 9 cirripede species to the cypris stage: *Megabalanus rosa* Pilsbry, 1916 ($n = 6$), *Austrominius* (= *Elminius*) *modestus* (Darwin, 1854) ($n = 6$), *Semibalanus balanoides* (Linnaeus, 1767) ($n = 6$), *Balanus crenatus* Bruguière, 1789 ($n = 11$), *Perforatus* (*Balanus*) *perforatus* (Bruguière, 1789) ($n = 5$), *Hesperibalanus fallax* (Broch, 1927) ($n = 9$), *Balanus balanus* (Linnaeus, 1758) ($n = 7$), *Balanus spongicola* Brown, 1844 ($n = 4$), and *Verruca stroemia* (O.F. Müller, 1776) ($n = 7$). All except the last two inhabit coastal hard-bottom communities, and all except *M. rosa* were collected from waters around the southern coast of England. The larvae were cultured as described in Moyse *et al.* (1995) and H. Al-Yahya (University of Swansea, unpubl. data). The preparation for scanning electron microscopy followed Moyse *et al.* (1995) and Al-Yahya *et al.* (2016). The SEM micrographs used for morphometric measurements were taken with either a JEOL-850 SEM or a JEOL-6335 SEM (Tokyo).

Choice of parameters

We were inspired by the approach of Al-Yahya *et al.* (2016) but extended our analysis to include many more features, including antennular segments 2–4 and their setae. Only the first segment was excluded from the analysis, because it carries no setae and was generally obscured from view in the SEM. The second antennular segment (as2) has an elongated shape. The short third segment (as3) carries the villus-covered AD; it forms the functional distal end of the appendage, because the short and semicylindrical fourth segment (as4) extends from it laterally (Fig. 1). Almost all antennular setae are located on the third and fourth segments; these setae

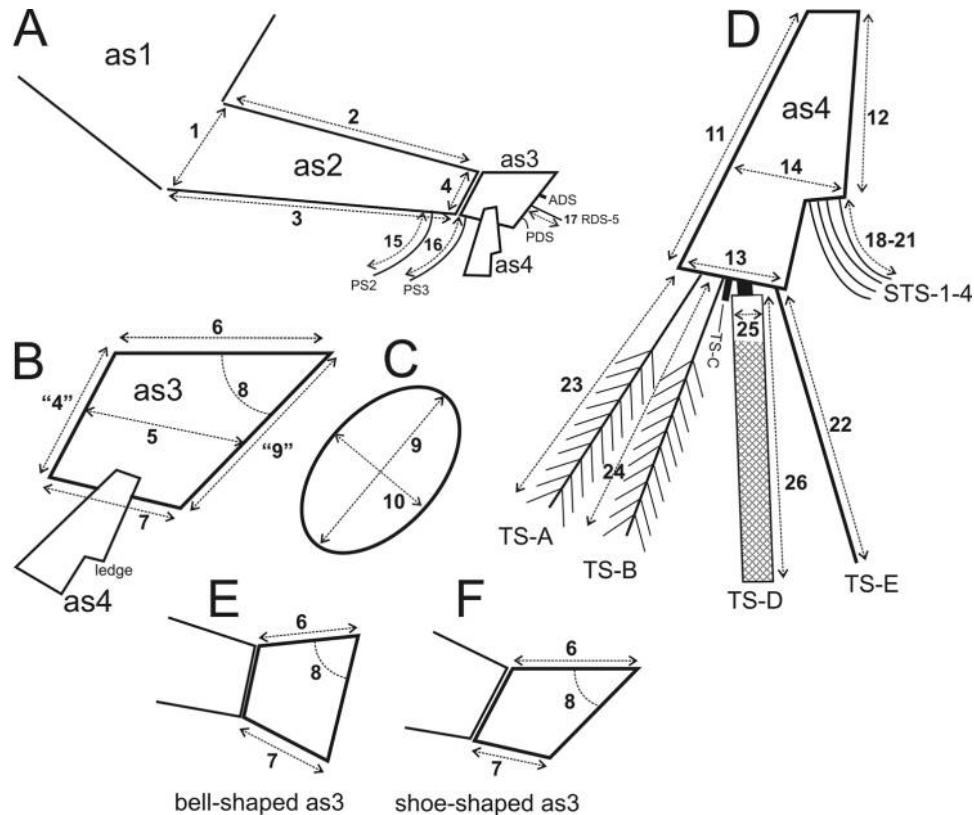


Figure 1. Schematic representation of the cypris antennule and the parameters measured in the analysis. The dorsal surface is also called preaxial, and the ventral surface is also called postaxial. (A) Antennule in lateral view. (B) Third antennular segment (as3) in lateral view with setae omitted. (C) Face-on view of the attachment disk on as3. (D) Fourth antennular segment (as4) and its setae. (E) Bell-shaped as3 in lateral view. (F) Shoe-shaped as3 in lateral view. Parameters measured: (1) basal width of second antennular segment (as2) at articulation to segment 1; (2) dorsal (preaxial) length of as2; (3) ventral (postaxial) length of as2; (4) distal width of as2 at articulation to as3; (5) length of as3 from the middle of the proximal joint to the middle of the attachment disk (AD); (6) dorsal (preaxial) length of as3; (7) ventral (postaxial) length of as3; (8) angle between the dorsal side of as3 and the plane of the AD; (9) longest diameter of the AD; (10) shortest diameter of the AD; (11) total length of as4; (12) length of as4 from the base to the ledge carrying the subterminal setae (STS); (13) width of as4 at the terminal platform; (14) width of as4 at the ledge; (15) length of postaxial seta 2 (PS2); (16) length of postaxial seta 3 (PS3); (17) length of radial disk seta 5 (RDS-5; other RDS setae not shown); (18–21) length of subterminal setae 1–4 (STS-1–4); (22) length of terminal seta E (TS-E); (23) length of terminal seta A (TS-A); (24) length of terminal seta B (TS-B); (25) width of subterminal seta D at the base of its sac-like part; (26) length of subterminal seta D. No independent record for the basal (4) and distal (9) widths of segment 3 were taken because these are identical to parameters 4 and 9. ADS, axial disk seta; PDS, postaxial disk seta.

have all been demonstrated to have sensory properties and are, therefore, sensilla (Nott and Foster, 1969; Walker *et al.*, 1987; Clare and Nott, 1994; Lagersson *et al.*, 2003; Høeg *et al.*, 2004; Maruzzo *et al.*, 2011). Nevertheless, we henceforth use the neutral term “seta” in order to conform to the existing terminology for antennular features set by Bielecki *et al.* (2009).

Scanning electron microscope procedure

During observation, the stubs were rotated and tilted to bring the cypris antennules into precise orientation for measurements as explained below. We attempted to record all parameters from both antennules in any individual cyprid, but

this was not always possible. In a few larvae we had to use suboptimal viewing angles for recording some parameters, and this could explain some or all of the outlying points in our multivariate analysis.

Segment shapes

Most measurements on as2 and as3 were recorded with the antennule observed in a perfect lateral or medial view. For AD measurements, we used perfect face-on views. In both live and preserved specimens, as4 can project at a range of angles from as3; hence, we oriented the specimens to observe this segment in a perfect lateral view.

Measurements of setae

All setae classified by Bielecki *et al.* (2009) were found in all species, except for a single one in *Verruca stroemia*. Most setae have a simple and slender shape, so length was the only critical parameter to record (except for terminal seta D [TS-D]). Since setae could be characteristically curved, we recorded their true length (Figs. 1–3), but we refrained from estimating curvatures because some setae are known to be very flexible in live cyprids (Maruzzo *et al.*, 2011) and their shape is also heavily influenced when undergoing preparation for scanning electron microscopy. For length measurements, we positioned the specimen so that the particular seta had its greatest extension over the screen. Measurements were carried out from stored micrograph files based on the scale and magnification given on images. A few setae deviated from a simple shape. The TS-D on the fourth segment was an elongated sac with a characteristic surface ornamentation of cuticular reinformant ribs (Figs. 2D, 3D). The ornamentation pattern can vary interspecifically and can also shift abruptly along the length of the seta, but we did not attempt to quantify this issue (Fig. 3D). Terminal setae A and B (TS-A + B) were measured separately but turned out to be mutually similar in all species. They were always fitted with numerous side branches (ribbon-like setules)

forming a plumose seta (Fig. 3C, D). It would have been desirable to record both the length and the separation distance of these setules, but they almost always became twisted in SEM preparations and were therefore not practically measurable. The setae on the AD were hard to measure accurately. Their basal part was obscured to various degrees by either the carpet of cuticular villi or the velum or skirt surrounding the disk; entire such disk setae could be totally obscured from view in some specimens (Bielecki *et al.*, 2009). Therefore, we omitted measurements of the postaxial disk seta, the axial disk seta, and all radial disk setae (RDS) except the medially placed RDS-5, which in most species was easy to measure because of its greater length (Fig. 3A). The tiny terminal seta C was always present but not measured.

Attachment disk features

In Figure 2E, the AD on as3 is covered by a carpet of minute cuticular villi, which can vary in density, length, and thickness (Nott, 1969; Moyse *et al.*, 1995; Aldred *et al.*, 2013), but Al-Yahya *et al.* (2016) found problems in attempting to quantify these parameters. In our micrographs, the AD is often prone to bulging parts, making it difficult to observe and count the min-

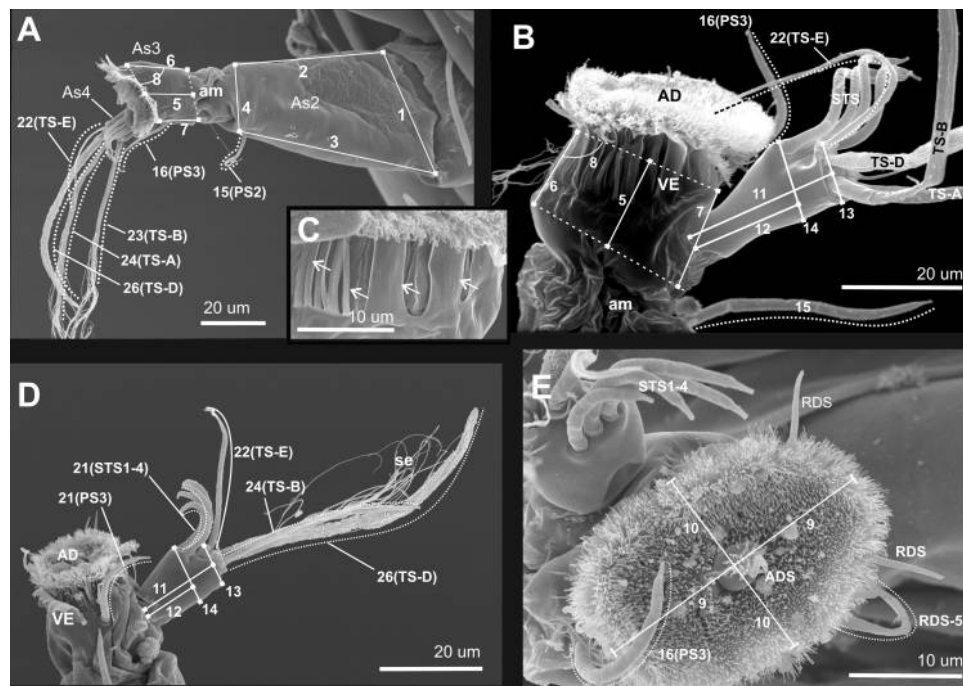


Figure 2. Selected SEM micrographs illustrating the parameters used in the multivariate statistical analysis. (A) *Verruca stroemia*; whole antennule in medial view; note the shoe shape of the third antennular segment (as3) showing that the attachment disk is ventrally angled. (B) *Semibalanus balanoides*; third (as3) and fourth (as4) antennular segments in lateral view; as3 is near symmetrical and bell shaped, with a distally facing attachment disk (AD); the dotted lines are not measured, since they are similar in value to parameters 4 and 9. (C) Detail of velum in *S. balanoides*; the velar filaments are very elongated but varying in width. (D) *Balanus balanus*; ventral view of as3 and as4. (E) *Perforatus perforatus*; face-on view of the AD, here with a slightly elongated outline. ADS, axial disk seta; am, arthrodial membrane; As2–4, antennular segments 2–4; PS2, postaxial seta 2; PS3, postaxial seta 3; RDS, radial seta; se, setules; STS1–4, subterminal setae 1–4; TS-A–E, terminal setae A–E; VE, velum.

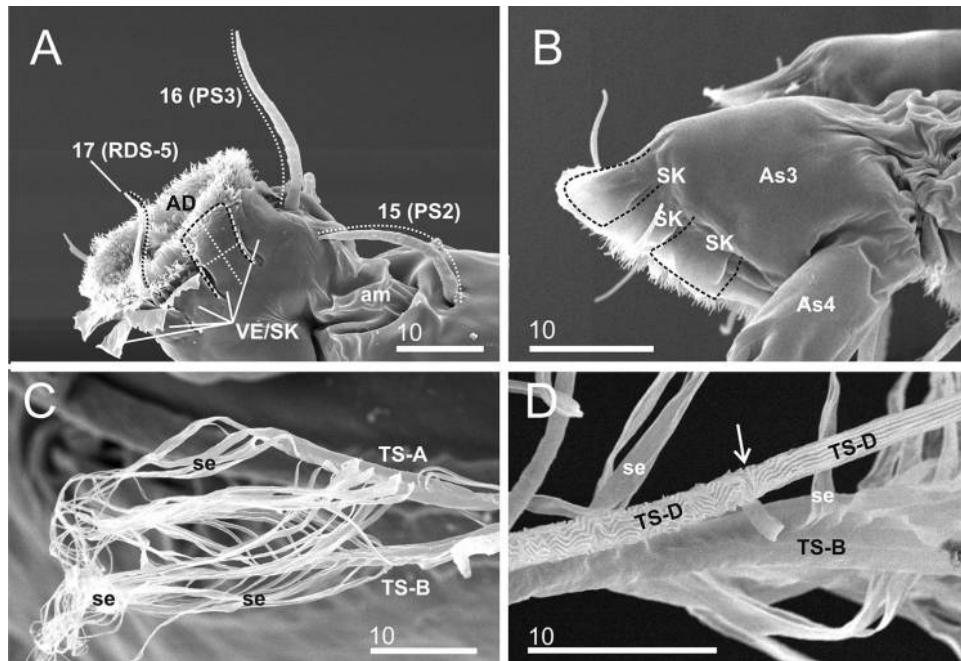


Figure 3. Selected SEM micrographs illustrating variation in antennular structures. (A) *Balanus balanus*; medial view of the third antennular segment (as3): the filaments (VE/SK) bordering the attachment disk (AD) are intermediate in shape between those of a velum and a skirt; the photo also shows radial seta 5 (RDS-5) in its full extent for accurate measurement. (B) *Verruca stroemia*; lateral view of the shoe-shaped third segment (as3); the AD bordered by a typical skirt (SK) consisting of low, broad cuticular flaps. (C) *Austrominius (=Elminius) modestus*; terminal setae A and B (TS-A+B) with numerous long ribbon-like setules diverging bilaterally from the distal part, but as here usually somewhat entangled with each other after SEM preparation. (D) *Austrominius (=Elminius) modestus*; close-up of terminal seta D (TS-D) highlighting the abrupt shift in ornamentation along its course (arrow); note the ribbon-like setules on TS-A. am, arthrodial membrane; As3–4, antennular segments 3–4; TS-A+B, terminal setae A and B; PS2–3, postaxial setae 2 and 3; se, setules; SK, skirt; VE, velum.

ute villi in a way suitable for statistical analysis, so this is omitted from our analysis. We recorded whether the disk is surrounded by a velum or a skirt (Al-Yahya *et al.*, 2016), but as presence or absence only, so this information forms no part of the multivariate analysis. A typical velum (Fig. 2B) is a sheet formed by a series of long but narrow cuticular filaments that are attached on the side of the segment some distance from the perimeter of the disk. In contrast, a true skirt (Fig. 3B) is attached at the very perimeter of the disk and consists of a series of low but broad cuticular flaps (Moyse *et al.*, 1995; Al-Yahya *et al.*, 2016; Figs. 2, 3). A quantification in terms of attachment position, numbers, length, and width of these filaments and flaps would have been desirable, but this was also impractical because they easily become distorted in preparation for the SEM.

Parameters measured

The 26 antennular parameters recorded are illustrated schematically in Figure 1 (see Table S1, available online, for raw data of measurement). Figures 2 and 3 illustrate how the parameters were estimated on actual SEM micrographs and also serve to highlight some differences between the currently

studied species. Note that the distal width of as2 as seen in lateral or medial view is always similar to the proximal width of as3; hence, we recorded only the first as parameter 4. Similarly, the distal width of as3 in lateral or medial view equates with that of the long axis of the AD seen face-on, and, accordingly, only the latter was recorded as parameter 9. In the multivariate analysis, we used the ratio of parameters 6 to 7 instead of their individual values because this ratio can be directly affected by the shape of as3.

Multivariate analysis

To compare variations in cyprid antennular morphology, a total of 25 quantitative parameters in the third and fourth segments were selected for analysis (note that characters 6 and 7 were used as a ratio in the analysis, so in total 25 characters, instead of 26, were used in the multivariate analysis; see details in Fig. 1). To remove variation due to the interspecific differences of size, all length measurements were divided by the mean length of cyprids (for the number of samples used for multivariate analysis, see Larval culture and SEM preparation, above). Variations in the parameter in antennules among species were analyzed using multivariate analysis (PRIMER 6,

Plymouth Routines in Multivariate Analysis; Clarke, 1993). Data were square-root transformed prior to analysis, and Euclidean distance was used for similarity matrix calculation. Nonmetric multidimensional scaling (nMDS) was conducted to generate the two-dimensional plots of the antennular parameters between barnacle species. Analysis of similarity (ANOSIM) was conducted to test for differences in antennular parameters between species. Under ANOSIM, the degree of similarity between pairs can be indicated by *R*-values in the Global test, in which *R* ranged from 0 to 1, where 0 indicates high similarity and 1 indicates low similarity. Chan *et al.* (2007a, b) have demonstrated the utility of this multivariate technique to discriminate the scutum and tergum parameters among barnacle species. Similarity percentage (SIMPER) analysis was conducted to examine the parameters that contributed to the differences among species (see Chan *et al.*, 2007b).

Results

Scanning electron microscopy analysis

The SEM micrographs showed that the antennular structure was surprisingly similar in almost all of the investigated species. Most significantly, mere inspection of the SEM photos revealed no obvious differences in the structure of setae, neither among the hard-bottom balanomorphans nor between these and the two remaining species. All of the setae found and classified by Bielecki *et al.* (2009) in *Megabalanus rosa* were present in the nine species and with virtually the same relative positions and morphologies. This is also true for the setae on the AD that were excluded from the multivariate analysis. The only exception was *Verruca stroemia*, where the RDS-5 is not exceptionally longer than the other RDS. We particularly emphasize that all species have exactly the same setation on the fourth segment, which extends laterally from the third segment and during settlement performs a sweeping motion that increases the substrate area probed by the exploring cyprid (Clare and Nott, 1994; Maruzzo *et al.*, 2011).

The most striking difference between the species concerned was the shape and structure of the third antennular segment: the attachment organ. In both *Balanus spongicola* and *V. stroemia*, the shape of the third segment is somewhat shoe shaped in lateral view, with the dorsal (preaxial) side of the segment longer than the ventral (postaxial) side. The result of this is a ventrally angled AD with an elongated oval outline when viewed face-on. All of the hard-bottom balanomorphans had a third segment that was almost symmetrically bell shaped and a distally facing AD with a near-circular outline.

Statistical analysis

The impression from the SEM micrographs was confirmed by the multivariate analysis of the structures measured, because the species fell into two clearly separated clusters. ANOSIM showed significant differences for the species included in the

analysis ($P < 0.05$, $R = 0.43$). Cluster A was composed of *V. stroemia* and the sponge-associated *B. spongicola*; ANOSIM indicated no significant differences between them (Table A1). Cluster B included all the balanomorphans from hard substrata in the coastal zone (Fig. 4). Most of the species within cluster B had no significant differences in antennule parameters (Table A1). However, a pairwise comparison of the *R*-values between cluster A and cluster B revealed that about half ranged from 0.9 to 1.0. Pairwise comparisons of species pairs within cluster B ranged from 0.3 to 0.7 (Table A1). SIMPER analysis showed that two parameters, the ratio between the dorsal and ventral length of as3 and the angle subtended between the dorsal side and the attachment disk, are the key parameters that contribute >40% of the differences between cluster A and cluster B. Within cluster B, the angle between the dorsal side of as3 and the plane of the AD is the key parameter, contributing >20% of the differences in significant species pairs (Table A1).

Velum and skirt

Our SEM photos indicated that velum and skirt are not nearly as distinct from each other as was stated by Al-Yahya *et al.* (2016). A typical velum with numerous thin filaments (Fig. 2B, C) was found in *Semibalanus balanoides*, while a typical skirt consisting of broad flaps was found in *B. spongicola* and *V. stroemia* (Fig. 3B). But some species had structures circumscribing the AD that were intermediate between these two extremes. *Balanus balanus* (Fig. 3A) had filaments or flaps that were rather few in number, almost square in shape, and attached closer to the disk perimeter than in, for example, *S. balanoides*. Thus, typical vela and skirts *sensu* Al-Yahya *et al.* (2016) may be extreme versions of the same general structure.

Discussion

In our multivariate analysis of cypris antennular morphology, all balanoidean species from coastal hard-bottom communities formed a single cluster, clearly separated from a cluster formed by the balanoidean *Balanus spongicola* and the non-balanomorph *Verruca stroemia*. These two species inhabit entirely different substrata. *Balanus spongicola* is normally epibiotic in marine sponges, although occasionally found on physical substrata, while *V. stroemia* inhabits deeper waters and is normally epibiotic, although found on a wide variety of organisms (Southward and Crisp, 1963; Southward, 2008).

Inspection of the SEM micrographs showed that the antennular setation is almost identical in number and structure in all species examined, so it is likely that the separation between the hard-bottom forms (cluster B) and *B. spongicola* and *V. stroemia* (cluster A) is primarily due to parameters 1–10, concerning the shape of the segments. Both *V. stroemia* and *B. spongicola* have a third segment that is shoe shaped, while the hard-bottom forms have a symmetrically bell-shaped segment, a difference also found among the species studied by

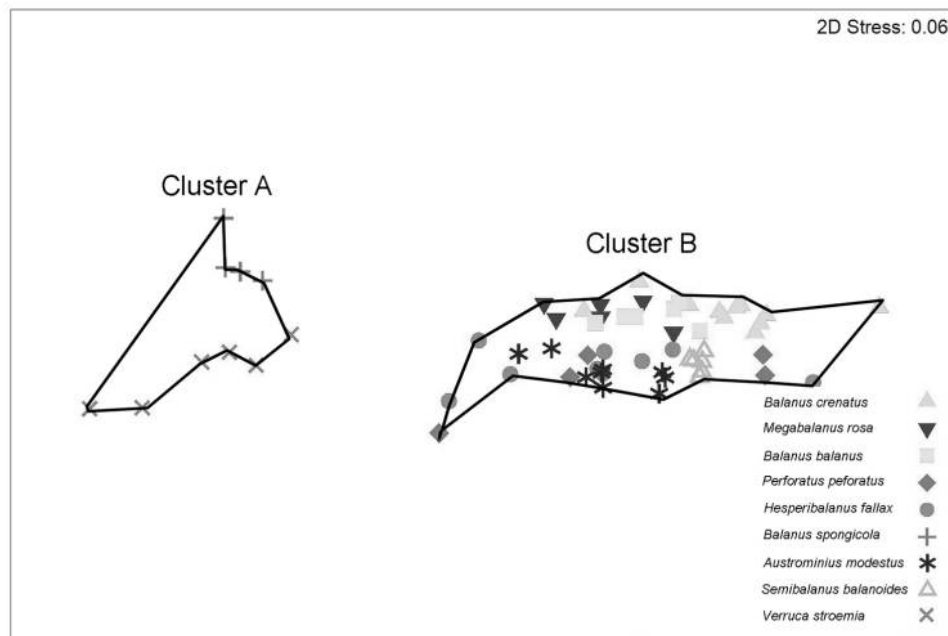


Figure 4. Nonmetric multidimensional scaling plot of 25 parameters (note that characters 6 and 7 were used as a ratio in the analysis) measured from antennular morphology in cyprids of *Verruca stroemia* and 8 species of balanomorphan barnacles. Cluster A contains *V. stroemia* and *Balanus spongicola*. Cluster B contains all the remaining balanomorphan species, all from hard-bottom habitats.

Moyse *et al.* (1995) and Chen *et al.* (2013). In their study comprising species from a wide range of taxa and habitats, Al-Yahya *et al.* (2016) suggested that a shoe-shaped third segment surrounded by a skirt is associated with an epibiotic habitat, while a bell-shaped segment surrounded by a velum is associated with a hard-bottom habitat; but their statistical analysis failed to adequately support this claim. It is nevertheless striking that a bell-shaped third segment has only been found in cyprids from hard-bottom balanomorphans and in the very few pedunculated barnacles from this same habitat, namely, *Pollicipes pollicipes* and *Capitulum mitella* (Moyse *et al.*, 1995; Rao and Lin, 2014; Al-Yahya *et al.*, 2016). This suggests that this segment shape is indeed associated with hard bottoms; but a detailed morphometric analysis, as in the present paper, that also includes *P. pollicipes*, *C. mitella*, and some of the numerous hard-bottom-inhabiting species from the balanomorphan superfamilies Chthamaloidea and Corunuloidea, is needed to further substantiate this claim. The relation between a velum and hard-bottom habitats is more dubious, because we found velum and skirt not to be very clearly separated in structure. Yet it is again striking that species from very high-energy, rocky intertidal habitats (*C. mitella*, *P. pollicipes*, *Semibalanus balanoides*, and species of *Chthamalus* and *Tetracita*) always seem to have not only a bell-shaped as3 but also a typical velum consisting of numerous long and thin filaments (Moyse *et al.*, 1995; Chan, 2003; Al-Yahya *et al.*, 2016; this study and our unpublished SEM data). In contrast, both *B. spon-*

gicola and *V. stroemia* have a typical skirt consisting of broad and low cuticular flanges. Here we wish to emphasize that little variation was found in the antennular structure among cyprids of balanomorphan species from coastal hard-bottom habitats. These species are also potentially fouling barnacles, and while we did not include the model species *Amphibalanus* (= *Balanus*) *amphitrite* in the present analysis, the detailed description in Glenner and Høeg (1995) shows that its antennular structure is exactly as in the other hard-bottom species studied here.

In conclusion, our analysis and previous studies show that there is significant variation in cypris antennular structure among cirripedes. This includes both the specific array of setae and the shape and detailed structure of the attachment organ, but the extent to which this structural variation is correlated with differences in habitat and settlement remains somewhat uncertain (Glenner *et al.*, 1989; Glenner and Høeg, 1995; Moyse *et al.*, 1995; Blomsterberg *et al.*, 2004; Kolbasov and Høeg, 2007; Brickner and Høeg, 2010; Chen *et al.*, 2013; Rao and Lin, 2014; Al-Yahya *et al.*, 2016). Nevertheless, the present analysis and the results in Al-Yahya *et al.* (2016) clearly show that species from coastal hard-bottom habitats have a unique and almost identical antennular structure. This agrees with Di Fino *et al.* (2014), one of the very few comparative studies of settlement biology in balanomorphans, which, contrary to some earlier claims, found no difference in the reaction to settlement cues between *Amphibalanus* (*Balanus*) *improvisus* and

A. amphitrite. In the absence of structural differences between cyprids, studies on settlement in hard-bottom-inhabiting balanomorphan species, which are also highly important as marine foulers, should continue to focus on refined experimental approaches (Aldred and Clare, 2008, 2009). One difficult but very promising avenue might well be electrophysiological experiments with cypris models that could lead to insight into the relation between sensory input and the resulting behavioral response (Harrison and Sandeman, 1999).

Acknowledgments

The authors wish to dedicate this paper to our friend Dr. Graham Walker, formerly at the Marine Science Laboratories Menai Bridge, and to our recently departed colleague, Dr. John Moyse, formerly at the University of Swansea, who understood the intimate relation between the structure and biology of cirripede larvae. The study was financed by grants to JTH from the Carlsberg Foundation, the Danish Agency for Independent Research (FNU), and the Villum Foundation, and a Senior Investigator Award to BKKC from the Academia Sinica.

Literature Cited

- Aldred, N., and A. S. Clare. 2008. The adhesive strategies of cyprids and development of barnacle-resistant marine coatings. *Biofouling* **24**: 351–363.
- Aldred, N., and A. S. Clare. 2009. Mechanisms and principles underlying temporary adhesion, surface exploration and settlement site selection by barnacle cyprids: a short review. Pp. 43–65 in *Functional Surfaces in Biology*, S. N. Gorb, ed. Springer, Berlin.
- Aldred, N., J. T. Høeg, D. Maruzzo, and A. S. Clare. 2013. Analysis of the behaviours mediating barnacle cyprid reversible adhesion. *PLoS One* **8**: e68085.
- Al-Yahya, H., H.-S. Chen, B. K. K. Chan, R. Kado, and J. T. Høeg. 2016. Morphology of cyprid attachment organs compared across disparate barnacle taxa: Does it relate to habitat? *Biol. Bull.* **231**: 120–129.
- Anderson, D. T. 1994. *Barnacles: Structure, Function, Development and Evolution*. Chapman & Hall, London.
- Bertness, M. D., S. D. Gaines, and S. M. Yeh. 1998. Making mountains out of barnacles: the dynamics of acorn barnacle hummocking. *Ecology* **79**: 1382–1394.
- Bielecki, J., B. K. K. Chan, J. T. Høeg, and A. Sari. 2009. Antennular sensory organs in cyprids of balanomorphan cirripedes: standardizing terminology using *Megabalanus rosa*. *Biofouling* **25**: 203–214.
- Blomsterberg, M., J. T. Høeg, W. B. Jeffries, and N. C. Lagersson. 2004. Antennular sensory organs in cyprids of *Octolasmis angulata* and three species of *Lepas* (Crustacea: Thecostraca: Cirripedia: Thoracica): a scanning electron microscopy study. *J. Morphol.* **200**: 141–153.
- Brickner, I., and J. T. Høeg. 2010. Antennular specialization in cyprids of coral associated barnacles. *J. Exp. Mar. Biol. Ecol.* **392**: 115–124.
- Chan, B. K. K. 2003. Studies on *Tetraclita squamosa* and *Tetraclita japonica* (Cirripedia: Thoracica). II. Larval morphology and development. *J. Crustac. Biol.* **23**: 522–547.
- Chan, B. K. K., L. M. Tsang, and K. H. Chu. 2007a. Cryptic diversity of the *Tetraclita squamosa* complex (Crustacea: Cirripedia) in Asia: description of a new species from Singapore. *Zool. Stud.* **46**: 46–56.
- Chan, B. K. K., L. M. Tsang, and K. H. Chu. 2007b. Morphological and genetic differentiation of the acorn barnacle *Tetraclita squamosa* (Crustacea, Cirripedia) in East Asia and description of a new species of *Tetraclita*. *Zool. Scr.* **36**: 79–91.
- Chen, H.-N., J. T. Høeg, and B. K. K. Chan. 2013. Morphometric and molecular identification of individual barnacle cyprids from the wild plankton: an approach to detect fouling and invasive barnacle species. *Biofouling* **29**: 133–145.
- Clare, A. S., and J. A. Nott. 1994. Scanning electron microscopy of the fourth antennular segment of *Balanus amphitrite amphitrite*. *J. Mar. Biol. Assoc. U.K.* **74**: 967–970.
- Clarke, K. R. 1993. Nonparametric multivariate analysis of changes in community structure. *Aust. J. Ecol.* **18**: 117–143.
- Di Fino, A., L. Petrone, N. Aldred, T. Ederth, B. Liedberg, and A. S. Clare. 2014. Correlation between surface chemistry and settlement behaviour in barnacle cyprids (*Balanus improvisus*). *Biofouling* **30**: 143–152.
- Glenner, H. 1999. Functional morphology of the cirripede cypris: a comparative approach. Pp. 161–187 in *Barnacles: The Biofoulers*, M.-F. Thompson and R. Nagabhushanam, eds. Regency, New Delhi.
- Glenner, H., and J. T. Høeg. 1995. Scanning electron microscopy of cyprid larvae in *Balanus amphitrite amphitrite* (Crustacea: Cirripedia: Thoracica: Balanomorpha). *J. Crustac. Biol.* **15**: 523–536.
- Glenner, H., J. T. Høeg, A. Klysner, and B. Brodin Larsen. 1989. Cypris ultrastructure, metamorphosis and sex in seven families of parasitic barnacles (Crustacea: Cirripedia: Rhizocephala). *Acta Zool.* **70**: 229–242.
- Harrison, P. J. H., and D. C. Sandeman. 1999. Morphology of the nervous system of the barnacle cypris larva (*Balanus amphitrite* Darwin) revealed by light and electron microscopy. *Biol. Bull.* **197**: 144–158.
- Høeg, J. T., and O. S. Møller. 2006. When similar beginnings lead to different ends: constraints and diversity in cirripede larval development. *Invertebr. Reprod. Dev.* **49**: 125–142.
- Høeg, J. T., N. C. Lagersson, and H. Glenner. 2004. The complete cypris larva and its significance in thecostracan phylogeny. Pp. 197–215 in *Evolutionary Developmental Biology of Crustacea, Crustacean Issues Ser. 15*, G. Scholtz, ed. Balkema, Lisse, The Netherlands.
- Kolbasov, G. A., and J. T. Høeg. 2007. Cypris larvae of acrothoracican barnacles (Thecostraca: Cirripedia: Acrothoracica). *Zool. Anz.* **246**: 127–151.
- Lagersson, N., and J. T. Høeg. 2002. Settlement behavior and antennular biomechanics in cypris larvae of *Balanus amphitrite* (Crustacea: Thecostraca: Cirripedia). *Mar. Biol.* **141**: 513–526.
- Lagersson, N. C., A. L. Garm, and J. T. Høeg. 2003. Notes on the ultrastructure of the setae on the fourth antennular segment of the *Balanus amphitrite* cyprid (Crustacea: Cirripedia: Thoracica). *J. Mar. Biol. Assoc. U.K.* **83**: 361–365.
- Maruzzo, D., S. Conlan, N. Aldred, A. S. Clare, and J. T. Høeg. 2011. Video observation of antennular sensory setae during surface exploration in cyprids of *Balanus amphitrite*. *Biofouling* **27**: 225–239.
- Moyse, J., P. G. Jensen, J. T. Høeg, and H. Al-Yahya. 1995. Attachment organs in cypris larvae: using scanning electron microscopy. Pp. 153–178 in *New Frontiers in Barnacle Evolution, Crustacean Issues Ser. 10*, F. T. Schram and J. T. Høeg, eds. Balkema, Rotterdam.
- Nott, J. 1969. Settlement of barnacle larvae: surface structure of the antennular attachment disc by scanning electron microscopy. *Mar. Biol.* **2**: 248–251.
- Nott, J., and B. Foster. 1969. On the structure of the antennular attachment organ of the cypris larva of *Balanus balanoides* (L.). *Philos. Trans. R. Soc. Lond. B Biol. Sci.* **256**: 115–134.
- Pérez-Losada, M., M. Harp, J. T. Høeg, Y. Aчитuv, D. Jones, H. Watanabe, and K. A. Crandall. 2008. The tempo and mode of barnacle evolution. *Mol. Phylogenet. Evol.* **46**: 328–346.
- Pérez-Losada, M., J. T. Høeg, N. Simon-Blecher, A. Aчитuv, D. Jones, and K. A. Crandall. 2014. Molecular phylogeny, systematics and morphological evolution of the acorn barnacles (Thoracica: Sessilia; Balanomorpha). *Mol. Phylogenet. Evol.* **81**: 147–158.

- Rao, X. Z., and G. Lin. 2014. Scanning electron microscopy of the cypris larvae of *Capitulum mitella* (Cirripedia: Thoracica: Scalpellomorpha). *J. Mar. Biol. Assoc. U.K.* **94**: 361–368.
- Rees, D. J., C. Noever, J. T. Høeg, A. Ommundsen, and H. Glenner. 2014. On the origin of a novel parasitic-feeding mode within suspension-feeding barnacles. *Curr. Biol.* **24**: 1429–1434.
- Southward, A. J. 2008. *Barnacles: Keys and Notes for the Identification of British Species, Synopses of the British Fauna, N.S., 57*. Linnean Society of London, London.
- Southward, A. J., and D. J. Crisp. 1963. *Catalogue of Main Marine Fouling Organisms (Found on Ships Coming into European Waters)*, Vol. 1, *Barnacles*. Organisation for Economic Co-operation and Development, Paris.
- Thompson, M. F., and R. Nagabhushanam, eds. 1999. *Barnacles: The Biofoulers*. Regency, New Dehli.
- Walker, G., A. B. Yule, and J. A. Nott. 1987. Structure and function of balanomorph larvae. Pp. 307–328 in *Barnacle Biology, Crustacean Issues Ser. 5*, A. J. Southward, ed. Balkema, Rotterdam.

Appendix

Table A1

Pairwise comparison analysis in analysis of similarity and R-statistics for antennular features in cyprids from the nine investigated species of cirripedes

Species pairwise comparison	P-value	R-statistics
<i>Balanus crenatus</i> vs. <i>Megabalanus rosa</i>	<0.05	0.33
<i>Balanus crenatus</i> vs. <i>Balanus balanus</i>	NS	0.09
<i>Balanus crenatus</i> vs. <i>Balanus perforatus</i>	NS	0.26
<i>Balanus crenatus</i> vs. <i>Hesperibalanus fallax</i>	<0.05	0.33
<i>Balanus crenatus</i> vs. <i>Balanus spongicola</i>	<0.05	0.99
<i>Balanus crenatus</i> vs. <i>Verruca stroemia</i>	<0.05	0.90
<i>Balanus crenatus</i> vs. <i>Austrominius modestus</i>	<0.05	0.41
<i>Balanus crenatus</i> vs. <i>Semibalanus balanoides</i>	NS	0.08
<i>Megabalanus rosa</i> vs. <i>Balanus balanus</i>	NS	0.06
<i>Megabalanus rosa</i> vs. <i>Balanus perforatus</i>	NS	0.22
<i>Megabalanus rosa</i> vs. <i>Hesperibalanus fallax</i>	NS	0.01
<i>Megabalanus rosa</i> vs. <i>Balanus spongicola</i>	<0.05	1
<i>Megabalanus rosa</i> vs. <i>Verruca stroemia</i>	<0.05	0.72
<i>Megabalanus rosa</i> vs. <i>Austrominius modestus</i>	NS	0.14
<i>Megabalanus rosa</i> vs. <i>Semibalanus balanoides</i>	<0.05	0.67
<i>Balanus balanus</i> vs. <i>Balanus perforatus</i>	NS	0.18
<i>Balanus balanus</i> vs. <i>Hesperibalanus fallax</i>	NS	0.09
<i>Balanus balanus</i> vs. <i>Verruca stroemia</i>	<0.05	0.81
<i>Balanus balanus</i> vs. <i>Austrominius modestus</i>	<0.05	0.19
<i>Balanus balanus</i> vs. <i>Semibalanus balanoides</i>	<0.05	0.36
<i>Balanus balanus</i> vs. <i>Balanus spongicola</i>	<0.05	1
<i>Balanus perforatus</i> vs. <i>Verruca stroemia</i>	<0.05	0.64
<i>Balanus perforatus</i> vs. <i>Austrominius modestus</i>	<0.05	0.34
<i>Balanus perforatus</i> vs. <i>Semibalanus balanoides</i>	<0.05	0.48
<i>Balanus perforatus</i> vs. <i>Balanus spongicola</i>	<0.05	0.75
<i>Hesperibalanus fallax</i> vs. <i>Balanus spongicola</i>	<0.05	0.79
<i>Hesperibalanus fallax</i> vs. <i>Verruca stroemia</i>	<0.05	0.66
<i>Hesperibalanus fallax</i> vs. <i>Austrominius modestus</i>	NS	0.06
<i>Hesperibalanus fallax</i> vs. <i>Semibalanus balanoides</i>	<0.05	0.33
<i>Balanus spongicola</i> vs. <i>Verruca stroemia</i>	NS	0.066
<i>Balanus spongicola</i> vs. <i>Austrominius modestus</i>	<0.05	1
<i>Balanus spongicola</i> vs. <i>Semibalanus balanoides</i>	<0.05	1
<i>Verruca stroemia</i> vs. <i>Austrominius modestus</i>	<0.05	0.77
<i>Verruca stroemia</i> vs. <i>Semibalanus balanoides</i>	<0.05	0.59
<i>Austrominius modestus</i> vs. <i>Semibalanus balanoides</i>	<0.05	0.2

NS, not significant.